(21) Dunsmuir, J. T. R.; Lane, A. P. *J. Chem. Soc. A* **1974**, 404.
(22) Edwards, H. G. M.; Woodward, L. A.; Gall, M. J.; Ware, M. J. *Spectrochim. Acta, Sect. A* **1970**, *26* 287.
(23) Ferraro, J. R. *J. Coord. Chem.* **1976**, *5*, 101.
(24) Clark, R. J.; Dunn, T. M. *J. Chem. Soc. A* **1963**, 1198.
(25) Work in progress.
(26) Colthrum, N. B.; Daly, L. H.; Wiberley, S. E. "Introduction to Infrared and Raman Spectroscopy"; Academic Press: New York, 1975; p 282.
(27) Bellamy, L. J. "The Infrared Spectra of Complex Molecules"; Chapman and Hall: London, 1975; pp 267, 290.

Contribution from the Research School of Chemistry, Australian National University, Canberra, A.C.T., Australia 2600

Metal Complexes of Hemilabile Ligands. Reactivity and Structure of Dichlorobis(*o*-(diphenylphosphino)anisole)ruthenium(II)

JOHN C. JEFFREY*[1] and THOMAS B. RAUCHFUSS*[1]

Received January 26, 1979

The red complex $RuCl_2(PO)_2$ (**1**) (PO = *o*-(diphenylphosphino)anisole) crystallizes from dichloromethane/hexane as a solvate, $RuCl_2(PO)_2 \cdot CH_2Cl_2$, and has been characterized by a single-crystal X-ray structural analysis. The crystals have space group $P2_1/n$ with $a = 11.194$ (1) Å, $b = 28.294$ (4) Å, $c = 12.458$ (1) Å, $\beta = 95.50$ (1)°, $Z = 4$, $\rho_{obsd} = 1.40$ g/cm^3, and $\rho_{calcd} = 1.40$ g/cm^3. The complex is six-coordinate with trans chlorine and cis phosphorus donor atoms. The Ru–P distances of 2.217 (1) and 2.219 (1) Å, are similar to those found for apical phosphines in square-pyramidal ruthenium(II) complexes. The Ru–O distances of 2.299 (3) and 2.257 (3) Å are greater than that of the sum of the respective covalent radii, consistent with a weak Ru–O bond. **1** undergoes reversible electrochemical oxidation in acetone at 0.778 V vs. Ag/AgCl and chemical oxidation with $NOBF_4$ to afford the paramagnetic complex $[RuCl_2(PO)_2](BF_4)$ (**2**), characterized by its ESR spectrum. The room-temperature reaction of **1** with CO gives initially a fluxional monomeric complex, $RuCl_2(PO)_2(CO)$ (**4**), and then *all-trans*-$RuCl_2(PO)_2(CO)_2$ (**3**), via dissociation of the Ru–O bonds. Reaction of **1** with CO at elevated temperatures gives a new *cis*-dicarbonyl isomer, $RuCl_2(PO)_2(CO)_2$ (**5**), which has trans phosphines. Unlike **4**, complex **5** does not readily lose CO thermally; however, it is photochemically converted to a mixture of **3** and **4**. Closely related reactions are observed when **1** is treated with *tert*-butyl isocyanide and the species $RuCl_2(PO)_2(t\text{-BuNC})_2$ (**6**) and $RuCl_2(PO)_2(t\text{-BuNC})$ (**7**) were identified spectroscopically (and isolated for **6**). A reaction scheme rationalizing the formation of **3**, **4**, **5**, **6**, and **7** is presented and the results are discussed in light of the known work on phosphinoanisole–transition-metal complexes.

Introduction

Studies of the coordination chemistry of transition metal phosphines are useful in understanding the catalytic activity of this class of compounds. The majority of the catalytically useful group 8 metal ions contain triphenylphosphine, e.g., $RhCl(PPh_3)_3$, $Rh(H)CO(PPh_3)_3$, $RuHCl(PPh_3)_3$, and $Ru(H)(O_2CCH_3)(PPh_3)_3$.[2] This is largely a matter of convenience, other phosphines being air sensitive, expensive, or not available commercially. In the past few years, however, more complex phosphines have been found in many applications to be superior to triphenylphosphine. This is especially true in the area of asymmetric hydrogenation and hydrosilylation.[3-6]

For some time, we have investigated the chemistry of phosphine–amine and phosphine–ether ligands with the expectation that these ligands would bind well enough to allow isolation but would readily dissociate the "hard" ligand component, thus generating a vacant site for substrate binding.[7] We call these ligands *hemilabile*.

The ruthenium chelates derived from *o*-(diphenylphosphino)anisole, PO, are precursors to active hydrogenation and

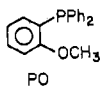

PO

isomerization catalysts and are related to the well-known Monsanto asymmetric catalysts, since both systems utilize phosphine–ether ligands. In a series of papers Shaw and co-workers have described the chemistry of other platinum metal complexes of phosphine anisoles.[9]

Experimental Section

All compounds described herein are air stable, both as solutions and in the solid state; nonetheless, reactions were performed in an inert atmosphere. Compounds were routinely recrystallized from dichloromethane; however, as it is often difficult to completely remove or stoichiometrically retain solvent in the crystalline solids obtained from it, the analyses are often only fair. Molecular weights were measured by vapor pressure osmometry in CH_2Cl_2. The electrochemical experiment was performed on apparatus described elsewhere.[11]

Improved Preparation of $RuCl_2(PO)_2$ (1). A 11.5-g sample of PO[12] (PO = *o*-(diphenylphosphino)anisole) was dissolved in 500 mL of boiling EtOH. A 4.5-g sample of Engelhardt "ruthenium trichloride" (35% Ru) was dissolved in 5 mL of H_2O in a steam bath and diluted with 10 mL of EtOH. The ruthenium solution was rapidly added to the phosphine solution at reflux and the brown mixture was boiled. After 30 min the solution was deep red and was allowed to cool overnight. The red crystals were filtered and washed with 100 mL of EtOH and 200 mL of Et_2O; yield 9.0 g.

Anal. Calcd for $C_{38}H_{34}Cl_2O_2P_2Ru$: C, 60.21; H, 4.50; Cl, 9.38; P, 8.20. Found: C, 60.6; H, 4.78; Cl, 9.36; P, 8.41.

$[RuCl_2(PO)_2]BF_4 \cdot CH_2Cl_2$ (2). A 187-mg sample of $Ru(PO)_2Cl_2$ (0.25 mmol) was suspended in MeCN and 30 mg of $NOBF_4$ was quickly added. The red suspension dissolved to give a homogeneous dark red solution which was evaporated. Crystallization from CH_2Cl_2 by the addition of Et_2O gave the product as the CH_2Cl_2 solvate.

Anal. Calcd for $C_{39}H_{36}BCl_4F_4O_2P_2Ru$: C, 50.40; H, 3.88; Cl, 15.30; P, 6.7. Found: C, 50.44; H, 4.04; Cl, 16.27; N, 0.00; P, 6.86.

***trans,trans,trans*-$RuCl_2(PO)_2(CO)_2$ (3).** A 220-mg sample of $Ru(PO)_2(CO)_2Cl_2$ was dissolved in 10 mL of CH_2Cl_2. After thorough saturation with CO for ca. 0.5 h, hexane was added in small portions while the CO atmosphere was maintained. After the complex had been precipitated, it was filtered and recrystallized from CH_2Cl_2–hexane under a CO atmosphere.

Anal. Calcd for $C_{40}H_{34}Cl_2O_2P_2Ru$: C, 59.11; H, 4.18; Cl, 8.7; P, 7.6. Found: C, 59.27; H, 4.48; Cl, 9.55; P, 7.61.

$Ru(PO)_2(CO)Cl_2$ (4). Samples of this complex were prepared as described previously.[7] For NMR purposes, it was found easier to prepare it in situ from *trans*-$RuCl_2(PO)_2(CO)_2$ (**3**) by displacement of the carbon monoxide by an argon purge; mol wt calcd 800, found 819.

***cis,trans,cis*-$RuCl_2(PO)_2(CO)_2$ (5).** $Ru(PO)_2Cl_2$, 300 mg, was heated in 20 mL of decane from 95 to 135 °C during 10 h in an atmosphere of CO. After the reaction period, the almost colorless solid was filtered and washed with pentane. The cream solid was

0020-1669/79/1318-2658$01.00/0

Table I. Crystal Data[a]

formula	$C_{39}H_{36}Cl_4O_2P_2Ru_1$ ($C_{38}H_{34}Cl_2O_2P_2Ru_1 \cdot CH_2Cl_2$)
fw	841.55
crystal class	monoclinic
cell dimensions[b] (23 ± 2 °C)	
a, Å	11.914 (1)
b, Å	28.297 (4)
c, Å	12.458 (1)
β, deg	95.50 (1)
unit cell vol, Å^3	3927.98
ρ_{obsd}, g cm^{-3}	1.42
ρ_{calcd}, g cm^{-3}	1.42
Z	4
space group	$P2_1/n$
crystal dimensions[c]	(01$\bar{1}$) to A, 0.108 mm; (010) to A, 0.138 mm; (011) to A, 0.108 mm; (0,*T*,0) to A, 0.138 mm; (120) to A, 0.188 mm; (120) to A, 0.188 mm
abs coeff cm^{-1}	7.61
Mo Kα radiation	no absorption correction applied

[a] Estimated standard deviations (in parentheses) in this and subsequent tables, and in the text, refer to the last significant digit(s). [b] At 23 ± 2 °C. [c] Crystal dimensions are quoted as the perpendicular distance of 16 faces ($h/2e$) from a common origin, A, within the xst.

Table II. Details of Data Collection

radiation	Mo Kα
wavelength, Å	0.709 26
takeoff angle, deg	3.0
monochromator	graphite xst
monochromator 2θ, deg	12.16
scan technique	θ–2θ scans
2θ scan speed, deg/min	2
individual scan range,[a] deg	(2θ − 0.65) to (2θ + 0.65 + Δ)
2θ range, deg	3–50.0
total background count time, s	20
std reflctns monitoring	3 every 97 reflections
std reflctns indices	(4,0,10), (0,20,0), (800)
crystal stability	7% isotropic decay
total no. of data collected	7789
no. of unique data with $I/\sigma(I) \geq 3$	5419 used
R_s[b]	0.016
R	0.039
R_w	0.055
std dev of unit wt	1.98

[a] The reflection scan range is asymmetric; the term Δ is the 2θ angular separation of the Kα_1 and Kα_2 components of the diffracted beam. [b] The statistical R_s factor is defined as $\Sigma\sigma_s(F_o)/\Sigma|F_o|$, where $\sigma_s(F_o) = \sigma(I)/C_{Lp}(2|F_o|)$, and C_{Lp} is the Lorentz-polarization correction.

extracted with CH_2Cl_2 and crystallized by the addition of MeOH followed by concentration; yield 235 mg as the CH_2Cl_2 solvate $[RuCl_2(PO)_2(CO)_2]\cdot CH_2Cl_2$, which was determined by ^1H NMR spectroscopy.

Anal. Calcd for $C_{41}H_{36}Cl_4O_2P_2Ru$: C, 55.78; H, 4.01; Cl, 16.01; P, 7.03; mol wt 967. Found: C, 55.17; H, 4.33; Cl, 16.25; P, 7.33; mol wt found 1063.

$RuCl_2(PO)_2$(*t*-BuNC)$_2$ (6). A 310-mg sample of $RuCl_2(PO)_2$ was suspended in 25 mL of benzene; 10 drops (~$^1/_2$ mL) of *t*-BuNC (*tert*-butyl isocyanide) was added to the red slurry, giving a golden solution which was allowed to stand for 5 min. A total of 75 mL of hexane was added and after scratching of the flask with a glass rod, yellow crystals formed which were filtered and washed with hexane; yield 335 mg. After being vacuum dried at 70 °C for 18 h, the material was analyzed.

Anal. Calcd for $C_{48}H_{52}Cl_2N_2O_2P_2Ru$: C, 62.47; H, 5.64; Cl, 6.72; N, 3.04; P, 7.69; mol wt calcd 922. Found: C, 62.66; H, 5.78; Cl, 6.35; N, 2.95; P, 7.76; mol wt found 832.

***trans*-$RuCl_2(PO)_2$(*t*-BuNC)(CO) (8).** A total of 5 drops of *t*-BuNC was added to a suspension of 200 mg of $RuCl_2(PO)_2(CO)Cl_2$ in 20 mL of $CHCl_3$. With stirring, the solid all dissolved and hexane was then slowly added to give a pale yellow crystalline product.

Anal. Calcd for $C_{45}H_{43}Cl_2NO_3P_2Ru$: C, 60.89; H, 4.96; N, 1.61; Cl, 8.17; P, 7.15; mol wt calcd 867. Found: C, 60.05; H, 5.20; N, 1.55; Cl, 9.76; P, 6.99; mol wt found 874.

Titration of 1 with *tert*-Butyl Isocyanide. A 37.5-mg sample of **1** (0.05 mmol) was dissolved in ca. 0.5 mL of $CDCl_3$ in an NMR tube. The 2.6-μL aliquots (ca. 0.025 mmol) of *t*-BuNC were added, the solutions were shaken, and the spectra were recorded within 5 min of addition. The spectra of the samples do not change on standing for 30 min. Similarly, reaction of equimolar quantities of **1** and **7** in $CDCl_3$ demonstrated that an equilibrium between **1**, **6**, and **7** is attained in less than 30 s.

Collection and Reduction of X-ray Intensity Data. Recrystallization of **1** from benzene/hexane, ethanol/hexane, or dichloromethane/hexane afforded deep red crystals as prisms or plates, all of which contained solvent of crystallization. The crystals from benzene or ethanol desolvate rapidly in air, becoming powdery and fractured and unsuitable for X-ray work. The dichloromethane solvate appeared not to desolvate and the NMR spectrum showed the solvent to complex ratio to be approximately 1:1. A suitable crystal was mounted on a quartz fiber with Araldite (an epoxy resin) and was completely coated with a thin film of Araldite to minimize possible solvent loss. There was no obvious deterioration of crystal quality during data collection. Approximate cell dimensions were obtained from preliminary Weissenberg (0*kl*, 1*kl*) and precession (*h*0*l*, *h*1*l*) photographs. Systematic absences of the type *h*0*l*, $h + l = 2n + 1$, and 0*k*0, $k = 2n + 1$, were observed and uniquely define the centrosymmetric monoclinic space group $P2_1/n$ a nonstandard setting of space group $P2_1/c$ (C_{2h}^5, No. 14). For $Z = 4$ there is no imposed crystallographic symmetry. Full details of the crystal data are listed in Table I.

Reflection data were collected on a Picker FACS-I fully automatic four-circle diffractometer with the crystallographic *a* axis and the instrumental Φ axis approximately coincident. Accurate cell dimensions and the crystal orientation matrix, together with their estimated standard errors, were obtained from the least-squares refinement of the 2θ, ω, χ, and Φ values of 12 carefully centered high-angle reflections (2θ > 40°).

Full details of the experimental conditions and data collection methods used are in Table II. During data collection, the intensities of three "standard" reflections showed a smooth isotropic decrease of ~7% (which was assumed to be 2θ independent) and the intensity data were corrected accordingly.

Reflection intensities were reduced to values of $|F_o|$,[13] and each reflection was assigned an individual estimated standard deviation $[\sigma(F_o)]$.[14] For this data set the instrumental "uncertainty factor"[15] (ρ) was assigned a value of $(0.002)^{1/2}$. Reflection data were sorted, equivalent reflections were averaged and reflections with $I/\sigma(I) < 3.0$ were discarded as being unobserved. Reflections for which the individual background measurements differed by more than 10σ were also discarded. The statistical *R* factor (R_s) for the 5419 reflections of the terminal data set was 0.016.

Solution and Refinement of the Structure. The structure was solved by conventional Patterson and difference Fourier syntheses and was refined by block-diagonal least-squares methods. Both the atomic scattering factors and the anomalous scattering factors (for the nonhydrogen atoms), were taken from the literature. A sample of the data was corrected for absorption by the analytical method;[14] since the maximum change in transmission coefficients was small, an absorption correction was not applied.

All nonhydrogen atoms were readily located from an iteration of least-squares and difference Fourier syntheses, but the temperature factors of the atoms in the dichloromethane solvent molecule (and, to a much smaller extent, some of the phenyl hydrogen atoms) were somewhat high. Close examination of an electron density map of this region showed single maxima for the chlorine and carbon atoms, but with a large spread of electron density. This is approximated by the high thermal parameters of these atoms, and a final difference Fourier synthesis showed only a single peak and a single trough of ~0.7 e/Å^3 in this region. Least-squares refinement of the site population parameters of the dichloromethane molecule showed no significant deviations from unity, confirming the NMR estimate of a 1:1 ratio of complex to solvent. In subsequent refinement, a unit population was assumed. Phenyl hydrogen atom contributions were included in the structure factor calculations (C–H = 0.95 Å,[15] $B_H = B_C$). These hydrogen atom coordinates and temperature factors were recalculated after every cycle of least-squares refinement. Two hydrogen atoms

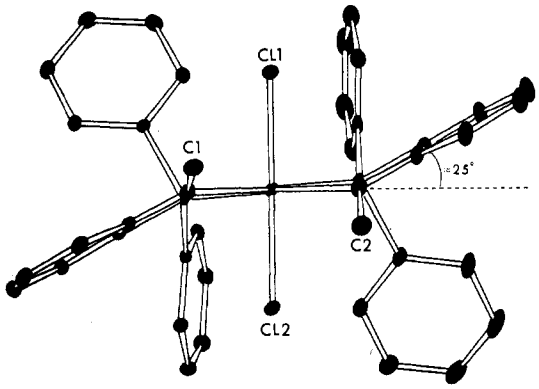

Figure 1. Perspective drawing of $RuCl_2(PO)_2$ approximately parallel to the chelate plane.

were located on each of the methoxyl methyl groups, thus allowing most probable coordinates for the remaining hydrogen atom on each methyl group to be calculated and included in the scattering model. A final cycle of diagonal matrix least-squares refinement with all nonhydrogen atoms anisotropic and with fixed contributions for all (except the CH_2Cl_2) hydrogen atoms gave $R = 0.039$ ($R_w = 0.055$). No individual parameter shift was greater than 0.1 of the corresponding estimated standard deviation. A final difference Fourier synthesis showed no peaks greater than ± 0.4 e/Å^3 (cf. a typical hydrogen atom was observed as ~ 0.5–0.6 e/Å^3) except for those previously noted in the vicinity of the dichloromethane solvent molecule. The standard deviation of an observation of unit weight, defined as $[\sum w(|F_o| - |F_c|)^2/(m-n)]^{1/2}$ (where m is the number of observations and n (=433) is the number of parameters varied), is 1.93. An examination of F_o and F_c shows no evidence of serious secondary extinction effects and there is no serious dependence of the minimized function on either $|F_o|$ or $\lambda^{-1} \sin \theta$. Final atomic positional and thermal parameters together with their estimated standard deviations (where appropriate) are listed in Table III. Final tables of structure factors have been deposited (supplementary material).

Computer Programs. The data reduction (SETUP), sorting (SORTER), Fourier (ANUFOR), least-squares (SFLS), and absorption correction (TOMPAB) programs have been described elsewhere.[16] The figures were produced by using ORTEP.[17] All calculations were carried out on the Univac-1108 computer of the Australian National University Computer Centre.

Results and Discussion

Description of the Structure. Perspective drawings of the molecule approximately parallel and perpendicular to the coordination plane containing the phosphorus and oxygen ligands are given in Figures 1 and 2. Principal bond distances and angles together with their standard deviations are listed in Table IV and the results of the mean plane calculations are in Table V.

The crystal structure consists of discrete monomeric molecular units which have approximately C_2 symmetry about the axis, which bisects the O(1)–Ru–O(2) (or P(1)–Ru–P(2)) angle. The complex has distorted octahedral geometry with trans chloride ligands and two coplanar PO chelates with cis oxygen and phosphorus donors. We note that the original assignment of mutually trans chelates is incorrect.[7] The coordination plane containing the two PO chelates is well defined and will be referred to as the principal coordination plane. There are significant in-plane angular distortions from the ideal interligand angles (90°) due to the restricted chelate bite angles of 78.81 and 79.47°. The P(1)–Ru–P(2) angle of 104.75 (3)° is larger than the O(1)–Ru–O(2) angle of 99.1 (1)°, presumably minimizing nonbonded interactions between the phenyl groups. The remaining coordination planes, P(1), Cl(1), O(2), Cl(2), Ru and P(2), Cl(1), O(1), Cl(2), Ru, are less well defined due to the Cl(1)–Ru–Cl(2) angle of 165.67 (3)°. Both chloride ligands are symmetrically bent away from the phosphorus atoms, thereby minimizing nonbonded interactions with the phenyl groups. As a further consequence

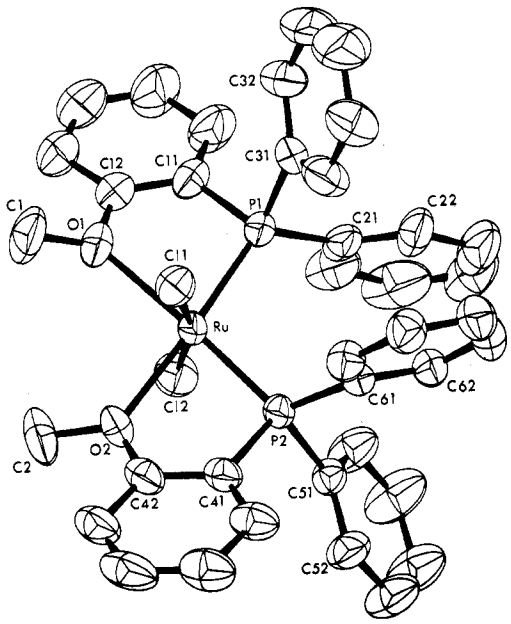

Figure 2. ORTEP drawing of $RuCl_2(PO)_2$ with thermal ellipsoids drawn at the 50% probability level.

of the steric crowding in **1**, the phenylene rings are all bent back, hinged about the P(1)–O(1) and P(2)–O(2) axes at an angle of ~25° (Figure 2); one phenylene ring lies above and the other below the principal coordination plane. A notable geometric consequence of this distortion is that it forces the methyl groups C(1) and C(2) onto opposite sides of the principal coordination plane with a C(1)–C(2) separation of 3.56 Å, thereby avoiding the severe nonbonded interactions which would arise if they lay in or closer to the principal coordination plane (cf.: the estimated separation of C(1)–C(2) for in-plane methyl groups is ~3.0 Å). For comparison, we note that the phenylene ring of the unique bidentate arsine ligand in the complex $RhCl_3(o\text{-}MeOC_6H_4AsMe_2)_2$, lies ~20° out of the analogous principal coordination plane.[18]

The cis Ru–P(1) and Ru–P(2) bond lengths of 2.217 (1) and 2.219 (1) Å, respectively, are identical within experimental error and, as expected, are considerably shorter than the distance observed in a number of six-coordinate Ru(II) complexes with mutually trans phosphines where values commonly range from 2.41 to 2.44 Å.[19,20] The average value of 2.218 (2) Å is also shorter than that observed in the cis phosphine complexes: *fac*-$[Ru_2Cl_3(PEt_2Ph)_6]^+$,[21] 2.318 (7) Å; *cis*-$Ru(SC_5H_4N)_2(PPh_3)_2$,[22] 2.319 (2) and 2.332 (2) Å for phosphines trans to chloride and nitrogen donors, respectively. *Indeed, the Ru–P distance in* **1** *is closest to that observed for apical phosphines in distorted square-pyramidal complexes where there is effectively no trans ligand competing for available electron density*; cf. $RuCl_2(PPh_3)_3$,[23] $Ru(H)Cl(PPh_3)_3$,[24] and $[RuS_2CCHPMe_2Ph)(PMe_2Ph)_3]PF_6$,[25] where the apical Ru–P distances are 2.23, 2.20, and 2.20 Å, respectively. Short Ru–P distances of 2.23 and 2.27 Å are also found in the complexes $RuH(O_2CCH_3)(PPh_3)_3$[26] and $RuH(O_2CH)(PPh_3)_3$,[27] where the unique phosphorus atoms are nominally trans to an anionic oxygen atom of the acetate or formate ligand. It has been suggested that in the formate complex the short Ru–P distance of 2.274 (13) Å results from the low trans influence of oxygen compared with that of phosphorus. In contrast, Skapski and Stevens[26] argue that the observed shortening is too great to result from this difference in trans influence and suggest that if the acetate or formate ligand be viewed as occupying only one coordination site, then the complex can be considered as quasi-five-coordinate. Hence, the unique phosphine would occupy the apical position of a

square pyramid with no trans competition for electrons and would resemble the previously noted complexes $RuHCl(PPh_3)_3$ and $RuCl_2(PPh_3)_3$. It is clear that ether oxygen atoms must have a very low trans influence, and it seems likely that such effects will also be important in the above acetate and formate complexes in which a similar shortening of the Ru–P bonds trans to anionic oxygen atoms is observed. This agrees with the work of Cetinkaya et al.,[28] who have compared the trans influence of a series of ligands for octahedral Rh(III) systems and, on the basis of the Rh–Cl distances trans to the ligand in question, established the order σ-alkyl > σ-phenyl > tertiary carbene > secondary carbene > tertiary phosphine > tertiary phosphite > tertiary arsine ~ π-olefin > chlorine ~ amine ~ pyridine > ROH.

The Ru–O(1) and Ru–O(2) distances of 2.299 (3) and 2.257 (3) Å are much longer than the sum of the covalent radii (1.99 Å),[29] which suggests that the oxygen atoms are only weakly coordinated. This is supported by the experimental observation that they are readily displaced by a variety of ligands in solution (vide infra). Comparisons with other available Ru–O distances are not entirely valid, since these generally involve anionic oxygen donors. However, we note that the distances in **1** are much longer than the values observed in a number of complexes in which the Ru–O bonds are not readily displaced: $Ru_2H(C_{10}H_9O)(CO)_6$, 2.10 Å;[30] $(Ru_2(O_2CC_3H_7)_4Cl)_n$,[31] 1.96–2.05 Å; $Ru_3O(O_2CCH_3)_6(PPh_3)_3$,[32] 1.92 and 2.06 Å. They are only slightly longer than the value of 2.246 (7) Å reported by Ibers et al. for the Ru–O distance in $RuH(CHC(CH_3)CO_2C_4H_9)(PPh_3)_3$, where the oxygen atom is trans to the hydride.[33] In this complex, the oxygen atom was considered to be weakly coordinated and could be readily displaced in solution. Similar observations were made for the analogous acetate and formate complexes in which the Ru–O distances are 2.29 (4) and 2.23 (3) Å and 2.20 (1) and 2.21 (1) Å, respectively. The weak Ru–O bonds in **1** support the proposition that they offer little trans competition for electron density, resulting in short Ru–P distances.

The Ru–Cl(1) and Ru–Cl(2) distances of 2.378 (1) and 2.392 (1) Å are essentially the same as those observed in a number of ruthenium(II) phosphines containing mutually trans chloride ligands; cf. $RuCl_2(PPh_3)_3$, 2.388 (7) Å;[23] $RuCl_3(p\text{-}N_2C_6H_9CH_3)(PPh_3)_2$, 2.390 (3) Å;[34] $RuCl_3(NO)(PMePh_2)_2$, 2.398 (7) Å.[35]

The PO ligand functions as an asymmetric bidentate chelate and its geometry is comparable with that of complexes of diphos, $o\text{-}C_6H_4(PMe_2)_2$. The chelate bite angles P(1)–Ru–O(1) and P(2)–Ru–O(2) of ~79° are at the lower end of the range of diphos complexes which range from 79 to 86°.[36] As noted earlier, the *o*-phenylene rings are bent out of the principal coordination plane by approximately 25° and similar behavior is observed in disphos complexes. The phosphorus atoms have the usual distorted geometry with the phenyl–P–phenyl angles averaging 103.3°. The oxygen atom geometry is consistent with sp^2 hybridization, and the oxygen atoms lie only 0.09 and 0.03 Å out of the Ru–C(1)–C(12) and Ru–C(2)–C(42) planes. The metrical details of the $-C_6H_4OCH_3$ portion of the PO ligands are very similar to other organic anisole derivatives.[37–40] In general, the methoxy group is found to be almost coplanar with the phenyl group, indicative of $2p\pi$ overlap with the aromatic ring. In **1**, the angles between the planes O(1)–C(1)–C(12) and O(2)–C(2)–C(41) and the planes of their respective phenylene rings are 156.7 and 164.1°. These angles are also consistent with appreciable $p\pi$ overlap. In contrast, the coordinated ether oxygen in $[Rh(CO)(Ph_2PCH_2CH_2OCH_2CH_2PPh_2)]PF_6$ was found to have distorted tetrahedral geometry.[41]

The dichloromethane solvent molecule sits in a cavity between symmetry related molecules and is not well behaved as evidenced by the high thermal motion and unrepresentative geometry. The average C–Cl distance of 1.76 Å is longer than that of 1.69 Å observed for an unusually well-ordered dichloromethane molecule in the complex $[RuCl(CO)(HN_2C_6H_5)(PPh_3)_2]ClO_4{\cdot}CH_2Cl_2$,[20] while the Cl(3)–C–Cl(4) angle at 96.2 (6)° is smaller than the value of 112.8 (7)° observed in the latter complex.

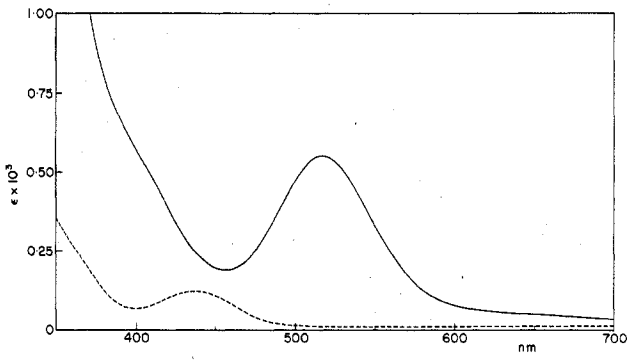

Figure 3. Electronic spectrum of $RuCl_2(PO)_2$ in $CHCl_3$ (solid line) and after purging with CO for 30 s (dashed line).

Properties and Reactivity of $RuCl_2(PO)_2$. The red color of **1** is due to an absorption maximum in the visible region at 517 nm (ϵ 550) both in solution (Figure 3) and as a Nujol mull. Most other hexacoordinated ruthenium(II)–phosphine complexes are yellow or colorless; cf. $RuCl_2(PR_3)_2L_2$ (L = PR_3,[42] CO,[43] PF_3,[44] RCN,[45] and olefin,[46,47]) and $RuCl_2(chelP_2)_2$ ($chelP_2$ = dppe,[48] diphos[49]). The related complex $RuCl_2(PN)_2$ (PN is *N,N*-dimethyl-*o*-(diphenylphosphino)aniline) is also red, as is the analogous complex of *o*-(diphenylphosphino)benzyl methyl ether.[7] Five-coordinate ruthenium(II) phosphines are more intensely colored than the coordinatively saturated analogues; $RuHCl(PPh_3)_3$ is purple while $RuCl_2(PPh_3)_3$ is black as a solid but brown in solution.[42]

Compound **1** undergoes reversible electrochemical oxidation in acetone at 0.778 V vs. Ag/AgCl; this value may be compared with those of $RuCl_2(diphos)_2$, 0.20 V, and $RuCl_2(diars)_2$, 0.17 V[49] (diphos = 1,2-bis(dimethylphosphino)benzene, diars = 1,2-bis(dimethylarsino)benzene). This oxidation was also performed chemically by using $NOBF_4$ as the oxidant, and the crystalline red-brown product $[RuCl_2(PO)_2]BF_4$, **2**, was isolated as the CH_2Cl_2 solvate. The X-band EPR spectrum of **2** in an acetone glass at 77 K has three absorptions at g = 1.58, 1.90, and 3.04. Similar values are reported for complexes of the type $RuCl_3L_3$ (L = PR_3, AsR_3).[50]

Owing to the presence of two weakly bound ether oxygen atoms, **1** is reactive toward a variety of ligands, although it is remarkably oxygen and heat stable. Earlier, we briefly reported the carbonylation of **1** and based our discussion on the isolation of $RuCl_2(PO)_2(CO)$ and infrared spectra.[14] We have now thoroughly reexamined this reaction relying on a broader range of analytical techniques and have isolated two new carbonylated products. Reaction of a solution of **1** with CO results in a rapid conversion to a mixture of two yellow carbonylated species (**3** and **4**). The disappearance of **1** is easily monitored visually (Figure 3) while the interconversions between the two carbonylated materials may be monitored by ^1H NMR or IR spectroscopy (Tables VI and VII). Carbonylation of 10^{-3} M nitromethane solutions of **1** results in little change (<3%) in its conductivity. Thorough purging of solutions of **1** with CO followed by precipitation of the product and recrystallization in an atmosphere of CO yields the yellow carbonyl **3**, which is assigned the all-trans geometry on the basis of the spectroscopic data. Solutions of **3** in the absence of CO, or better with an inert gas purge, convert to the monocarbonyl $Ru(PO)_2(CO)Cl_2$ (**4**).

Table III

(a) Atomic Coordinates and Anisotropic Temperature Factors for $RuCl_2(PO)_2$[a]

atom	x	y	z	atom	x	y	z
Ru	0.13278 (2)	0.13010 (1)	0.35304 (2)	C(34)	0.1966 (7)	0.3414 (2)	0.3490 (5)
P(1)	0.26390 (8)	0.18268 (4)	0.30350 (7)	C(35)	0.1826 (5)	0.3107 (2)	0.4303 (4)
P(2)	0.18218 (7)	0.11953 (3)	0.52803 (7)	C(36)	0.2023 (4)	0.2630 (2)	0.4146 (4)
Cl(1)	−0.01848 (8)	0.18441 (3)	0.39399 (8)	C(41)	0.0463 (3)	0.0933 (1)	0.5722 (3)
Cl(2)	0.24398 (10)	0.06617 (4)	0.28576 (8)	C(42)	−0.0321 (3)	0.0716 (1)	0.4940 (3)
O(1)	0.06449 (24)	0.14139 (10)	0.17489 (21)	C(43)	−0.1340 (4)	0.0480 (1)	0.5221 (4)
O(2)	−0.00120 (23)	0.07409 (9)	0.38914 (20)	C(44)	−0.1601 (4)	0.0477 (2)	0.6257 (4)
C(1)	−0.0591 (4)	0.1426 (2)	0.1337 (4)	C(45)	−0.0863 (4)	0.0703 (2)	0.7057 (4)
C(2)	−0.0604 (4)	0.0437 (2)	0.3098 (4)	C(46)	0.0165 (3)	0.0931 (1)	0.6782 (3)
C(11)	0.2536 (4)	0.1750 (2)	0.1569 (3)	C(51)	0.3023 (3)	0.0791 (1)	0.5802 (3)
C(12)	0.1505 (4)	0.1556 (1)	0.1074 (3)	C(52)	0.2955 (3)	0.0529 (1)	0.6733 (3)
C(13)	0.1315 (5)	0.1507 (2)	−0.0037 (3)	C(53)	0.3915 (4)	0.0255 (2)	0.7136 (3)
C(14)	0.2236 (6)	0.1642 (2)	−0.0641 (3)	C(54)	0.4949 (4)	0.0244 (2)	0.6640 (4)
C(15)	0.3266 (5)	0.1822 (2)	−0.0175 (4)	C(55)	0.5010 (4)	0.0497 (2)	0.5727 (4)
C(16)	0.3425 (4)	0.1880 (2)	0.0925 (3)	C(56)	0.4052 (4)	0.0771 (2)	0.5296 (3)
C(21)	0.4237 (3)	0.1762 (2)	0.3449 (3)	C(61)	0.2129 (3)	0.1705 (1)	0.6166 (2)
C(22)	0.4799 (4)	0.2060 (2)	0.4230 (3)	C(62)	0.3303 (3)	0.1831 (1)	0.6491 (3)
C(23)	0.5981 (4)	0.1987 (2)	0.4602 (4)	C(63)	0.3548 (3)	0.2242 (2)	0.7077 (3)
C(24)	0.6626 (4)	0.1634 (3)	0.4233 (5)	C(64)	0.2644 (4)	0.2524 (1)	0.7339 (3)
C(25)	0.6097 (4)	0.1340 (2)	0.3459 (5)	C(65)	0.1464 (4)	0.2401 (1)	0.7051 (3)
C(26)	0.4882 (4)	0.1405 (2)	0.3055 (4)	C(66)	0.1201 (3)	0.1991 (1)	0.6450 (3)
C(31)	0.2382 (3)	0.2462 (1)	0.3193 (3)	C(3)	0.2704 (15)	0.0315 (4)	0.0204 (7)
C(32)	0.2524 (6)	0.2780 (2)	0.2378 (4)	Cl(3)	0.1361 (5)	0.0216 (2)	−0.0652 (3)
C(33)	0.2312 (8)	0.3261 (2)	0.2541 (5)	Cl(4)	0.3149 (6)	−0.0272 (2)	0.0292 (4)

atom	β_{11}	β_{22}	β_{33}	β_{12}	β_{13}	β_{23}
Ru	0.00543 (2)	0.00091 (1)	0.00577 (2)	−0.00026 (1)	−0.00129 (2)	0.00016 (1)
P(1)	0.00670 (8)	0.00132 (1)	0.00553 (6)	−0.00066 (3)	−0.00119 (6)	0.00051 (2)
P(2)	0.00470 (7)	0.00089 (1)	0.00564 (6)	−0.00005 (2)	−0.00013 (5)	0.00016 (2)
Cl(1)	0.00636 (7)	0.00133 (1)	0.00933 (7)	0.00048 (3)	−0.00112 (6)	0.00045 (2)
Cl(2)	0.01081 (10)	0.00125 (1)	0.00883 (8)	0.00032 (3)	0.00069 (7)	−0.00039 (3)
O(1)	0.00881 (26)	0.00193 (5)	0.00727 (20)	−0.00079 (9)	−0.00301 (19)	0.00038 (7)
O(2)	0.00852 (24)	0.00118 (4)	0.00877 (20)	−0.00117 (8)	−0.00172 (18)	0.00007 (7)
C(1)	0.0104 (5)	0.0027 (1)	0.0101 (4)	0.0002 (2)	−0.0045 (4)	−0.0003 (2)
C(2)	0.0093 (4)	0.0013 (1)	0.0127 (4)	−0.0007 (1)	−0.0015 (3)	−0.0012 (1)
C(11)	0.0101 (4)	0.0017 (1)	0.0062 (3)	−0.0007 (1)	−0.0014 (3)	0.0006 (1)
C(12)	0.0121 (5)	0.0015 (1)	0.0065 (3)	−0.0009 (1)	−0.0020 (3)	0.0007 (1)
C(13)	0.0187 (7)	0.0025 (1)	0.0062 (3)	−0.0025 (2)	−0.0030 (4)	0.0007 (1)
C(14)	0.0241 (9)	0.0031 (1)	0.0056 (3)	−0.0022 (3)	−0.0013 (4)	0.0008 (1)
C(15)	0.0180 (7)	0.0038 (1)	0.0063 (3)	−0.0021 (3)	0.0014 (4)	0.0011 (2)
C(16)	0.0122 (5)	0.0030 (1)	0.0067 (3)	−0.0014 (2)	0.0005 (3)	0.0011 (1)
C(21)	0.0067 (3)	0.0023 (1)	0.0063 (3)	−0.0011 (1)	−0.0003 (2)	0.0017 (1)
C(22)	0.0083 (4)	0.0031 (1)	0.0065 (3)	−0.0017 (2)	−0.0012 (3)	0.0011 (1)
C(23)	0.0086 (4)	0.0046 (2)	0.0106 (4)	−0.0025 (2)	−0.0034 (4)	0.0022 (2)
C(24)	0.0062 (4)	0.0055 (2)	0.0155 (6)	−0.0016 (2)	−0.0016 (4)	0.0051 (3)
C(25)	0.0077 (4)	0.0040 (2)	0.0177 (7)	0.0013 (2)	0.0040 (4)	0.0041 (2)
C(26)	0.0089 (4)	0.0026 (1)	0.0112 (4)	0.0001 (2)	0.0018 (3)	0.0015 (2)
C(31)	0.0095 (4)	0.0012 (1)	0.0082 (3)	−0.0012 (1)	−0.0025 (3)	0.0006 (1)
C(32)	0.0263 (9)	0.0016 (1)	0.0083 (3)	−0.0027 (2)	−0.0014 (4)	0.0009 (1)
C(33)	0.0406 (14)	0.0014 (1)	0.0133 (5)	−0.0026 (3)	−0.0034 (7)	0.0016 (2)
C(34)	0.0306 (11)	0.0010 (1)	0.0166 (6)	−0.0008 (2)	−0.0024 (7)	0.0001 (2)
C(35)	0.0189 (7)	0.0014 (1)	0.0137 (5)	−0.0006 (2)	0.0007 (5)	−0.0003 (1)
C(36)	0.0131 (5)	0.0013 (1)	0.0105 (4)	−0.0009 (1)	0.0007 (4)	0.0006 (1)
C(41)	0.0052 (3)	0.0009 (1)	0.0082 (3)	0.0000 (1)	0.0008 (2)	0.0005 (1)
C(42)	0.0059 (3)	0.0010 (1)	0.0100 (3)	−0.0002 (1)	−0.0004 (3)	0.0007 (1)
C(43)	0.0067 (3)	0.0013 (1)	0.0141 (4)	−0.0007 (1)	−0.0011 (3)	0.0009 (1)
C(44)	0.0073 (4)	0.0018 (1)	0.0173 (5)	−0.0001 (1)	0.0026 (4)	0.0025 (2)
C(45)	0.0088 (4)	0.0020 (1)	0.0121 (4)	0.0003 (1)	0.0043 (3)	0.0012 (1)
C(46)	0.0081 (4)	0.0013 (1)	0.0089 (3)	0.0001 (1)	0.0020 (3)	0.0005 (1)
C(51)	0.0060 (3)	0.0010 (1)	0.0060 (2)	0.0002 (1)	−0.0005 (2)	0.0001 (1)
C(52)	0.0079 (4)	0.0017 (1)	0.0076 (3)	0.0006 (1)	0.0005 (3)	0.0010 (1)
C(53)	0.0118 (5)	0.0024 (1)	0.0089 (4)	0.0012 (2)	0.0000 (3)	0.0020 (1)
C(54)	0.0105 (5)	0.0028 (1)	0.0126 (5)	0.0029 (2)	0.0005 (4)	0.0021 (2)
C(55)	0.0090 (4)	0.0035 (1)	0.0114 (4)	0.0029 (2)	0.0027 (4)	0.0021 (2)
C(56)	0.0089 (4)	0.0023 (1)	0.0079 (3)	0.0016 (1)	0.0014 (3)	0.0012 (1)
C(61)	0.0067 (3)	0.0010 (1)	0.0047 (2)	−0.0002 (1)	0.0002 (2)	0.0001 (1)
C(62)	0.0069 (3)	0.0013 (1)	0.0061 (2)	−0.0005 (1)	0.0005 (2)	−0.0001 (1)
C(63)	0.0078 (3)	0.0017 (1)	0.0078 (3)	−0.0009 (1)	−0.0002 (3)	−0.0005 (1)
C(64)	0.0126 (4)	0.0013 (1)	0.0072 (3)	−0.0007 (1)	−0.0003 (3)	−0.0010 (1)
C(65)	0.0104 (4)	0.0013 (1)	0.0075 (3)	0.0007 (1)	0.0002 (3)	−0.0007 (1)
C(66)	0.0071 (3)	0.0012 (1)	0.0070 (3)	0.0001 (1)	−0.0005 (2)	−0.0002 (1)
C(3)	0.0935 (42)	0.0054 (3)	0.0139 (8)	0.0089 (10)	−0.0087 (16)	−0.0030 (4)
Cl(3)	0.0686 (9)	0.0069 (1)	0.0307 (5)	−0.0030 (3)	−0.0056 (6)	−0.0043 (2)
Cl(4)	0.0897 (14)	0.0078 (2)	0.0419 (8)	0.0079 (4)	0.0107 (9)	0.0040 (3)

Table III (*Continued*)

(b) Atomic Coordinates and Isotropic Thermal Factors for Hydrogen Atoms

atom	*x*	*y*	*z*	*B*, Å²	atom	*x*	*y*	*z*	*B*, Å²
H(13)	0.058	0.139	−0.037	7.2	H(46)	0.067	0.109	0.733	4.5
H(14)	0.213	0.161	−0.140	8.5	H(52)	0.225	0.054	0.710	4.7
H(15)	0.389	0.191	−0.061	8.4	H(53)	0.386	0.007	0.777	6.4
H(16)	0.415	0.201	0.125	6.6	H(54)	0.561	0.006	0.693	7.3
H(22)	0.437	0.231	0.451	6.1	H(55)	0.572	0.049	0.537	7.5
H(23)	0.635	0.219	0.514	8.7	H(56)	0.411	0.094	0.465	5.5
H(24)	0.744	0.159	0.451	10.1	H(62)	0.394	0.163	0.631	3.8
H(25)	0.655	0.109	0.319	9.0	H(63)	0.436	0.233	0.730	4.7
H(26)	0.452	0.120	0.251	6.5	H(64)	0.282	0.281	0.772	5.0
H(32)	0.277	0.267	0.171	7.9	H(65)	0.083	0.259	0.726	4.7
H(33)	0.241	0.348	0.198	11.2	H(66)	0.039	0.191	0.624	3.9
H(34)	0.182	0.374	0.359	9.7	H(1)	−0.108	0.137	0.191	6.8
H(35)	0.160	0.322	0.497	7.5	H(2)	−0.077	0.173	0.102	6.8
H(36)	0.191	0.241	0.471	5.7	H(3)	−0.074	0.119	0.081	6.8
H(43)	−0.185	0.032	0.468	5.4	H(4)	−0.021	0.045	0.246	5.7
H(44)	−0.230	0.032	0.644	6.6	H(5)	−0.058	0.012	0.336	5.7
H(45)	−0.106	0.070	0.778	5.9	H(6)	−0.142	0.053	0.295	5.7

[a] Anistropic thermal parameters were of the form $\exp[-(\beta_{11}h^2 + \beta_{22}k^2 + \beta_{33}l^2 + 2\beta_{12}hk + 2\beta_{13}hl + 2\beta_{23}kl)]$.

Table IV. Selected Distances (Å) and Angles (deg) in $RuCl_2(P(C_6H_5)_2(o\text{-}C_6H_4OCH_3))_2 \cdot CH_2Cl_2$

Ru-P(1)	2.219 (1)	P(2)-C(41)	1.825 (3)
Ru-P(2)	2.217 (1)	P(2)-C(51)	1.829 (3)
Ru-O(1)	2.299 (3)	P(2)-C(61)	1.835 (3)
Ru-O(2)	2.257 (3)	O(1)-C(1)	1.429 (5)
Ru-Cl(1)	2.378 (1)	O(1)-C(12)	1.396 (5)
Ru-Cl(2)	2.392 (1)	O(2)-C(2)	1.424 (5)
P(1)-C(11)	1.832 (4)	O(2)-C(42)	1.384 (5)
P(1)-C(21)	1.823 (4)	C(3)-Cl(3)	1.78 (1)
P(1)-C(31)	1.834 (4)	C(3)-Cl(4)	1.74 (1)
P(1)-Ru-O(2)	175.14 (7)	Ru-P(1)-C(31)	120.8 (1)
P(2)-Ru-O(1)	175.03 (7)	C(11)-P(1)-C(21)	103.7 (2)
Cl(1)-Ru-Cl(2)	165.67 (3)	C(11)-P(1)-C(31)	103.2 (2)
P(1)-Ru-P(2)	104.75 (3)	C(21)-P(1)-C(31)	103.2 (2)
P(1)-Ru-O(1)	78.81 (7)	Ru-P(2)-C(41)	102.4 (1)
P(1)-Ru-Cl(1)	97.46 (4)	Ru-P(2)-C(51)	122.5 (1)
P(1)-Ru-Cl(2)	91.68 (4)	Ru-P(2)-C(61)	120.1 (1)
O(2)-Ru-P(2)	79.47 (7)	C(41)-P(2)-C(51)	104.1 (2)
O(2)-Ru-O(1)	97.13 (9)	C(41)-P(2)-C(61)	104.6 (2)
O(2)-Ru-Cl(1)	84.87 (7)	C(51)-P(2)-C(61)	100.9 (2)
O(2)-Ru-Cl(2)	85.23 (7)	P(1)-C(11)-C(12)	117.7 (3)
Cl(1)-Ru-O(1)	86.54 (7)	P(1)-C(11)-C(16)	124.4 (3)
Cl(1)-Ru-P(2)	89.53 (3)	C(12)-C(11)-C(16)	117.8 (3)
Cl(2)-Ru-O(1)	84.43 (8)	O(1)-C(12)-C(11)	116.4 (3)
Cl(2)-Ru-P(2)	98.82 (3)	O(1)-C(12)-C(13)	121.5 (4)
Ru-O(1)-C(1)	124.8 (3)	C(11)-C(12)-C(13)	122.0 (4)
Ru-O(1)-C(12)	115.9 (2)	P(2)-C(41)-C(42)	117.1 (3)
Ru-O(2)-C(2)	124.0 (2)	C(42)-C(41)-C(46)	118.1 (3)
Ru-O(2)-C(42)	117.1 (2)	O(2)-C(42)-C(41)	116.2 (3)
C(2)-O(2)-C(42)	118.8 (3)	C(2)-C(42)-C(43)	123.1 (3)
Ru-P(1)-C(11)	102.6 (1)	C(41)-C(42)-C(43)	120.7 (4)
Ru-P(1)-C(21)	120.8 (1)	Cl(3)-C(3)-Cl(4)	96.2 (6)

The NMR data of **4** are consistent with a rapid equilibrium between two equivalent structures involving a five-coordinate intermediate via the process shown in eq 1. We favor a

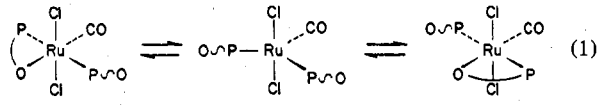
(1)

structure with trans phosphines for **4**, since it is a precursor to the all-trans dicarbonyl **3**, and another new cis dicarbonyl which also has trans phosphines (vide infra). We rule out chloride-bridged dimeric structures on the basis of the similarity of the Ru–Cl stretching frequencies of **1**, **3**, and **4** and the molecular weight in CH_2Cl_2 solutions. Attempts to slow the equilibrium (eq 1) to the NMR time scale failed, the ^1H NMR spectrum of **4** in CD_2Cl_2 being unchanged to −80 °C. On the basis of the dynamic equilibrium proposed for **4**, the chemical shift of the averaged methyl groups is expected to be intermediate between that of the coordinated chelate, τ 5.60 (**1**), and the uncoordinated ligand, τ 6.40 (PO). In fact, the ^1H chemical shift of the methyl resonance of **4** is peculiar in that it is upfield (τ 6.65) of both free PO and **3** (τ 6.49), respectively. Molecular models of this complex, however, demonstrate that, in the trans configuration, the coordinated methoxyl group is constrained within close proximity of the faces of the phenyl rings of the monodentate PO ligand and that the shielding by the ring current of these aromatic groups would cause the upfield shift. The steric crowding in **3** appears to be less than that in **4**; consequently, the methoxy groups of **3** are closer to the free ligand position. Similar effects are observed in the case of the isocyanide derivatives (vide infra).

The reaction of **1** with CO at elevated temperatures in alkane solvents yields a third, colorless compound, $RuCl_2(PO)_2(CO)_2$ (**5**), isomeric with **3**. The geometry of **5** is clearly defined by its spectroscopic data (Tables VI and VII); comparison of the ν(Ru–Cl) values with previous work indicates that these are appropriate for chloride trans to CO.[51,52] These data, together with the osmometric measurements, require the trans,cis,cis (C_{2v}) geometry for **5**. In contrast with

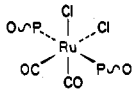
5

3, **5** does not readily lose CO, probably reflecting the relative trans influences or π-acceptor abilities of CO and Cl. However, **5** is photochemically reactive; UV photolysis of **5** in CH_2Cl_2 causes a yellowing of the solution and the appearance of two new bands at 1995 and 2020 cm^{-1} consistent with the formation of **3** and **4** (eq 2).

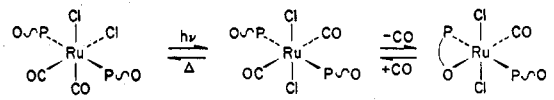
(2)

The reaction of **1** with excess *tert*-butyl isocyanide (*t*-BuNC) yields the yellow complex $RuCl_2(PO)_2(t\text{-BuNC})_2$ (**6**). IR (Table VII), ^1H and ^{31}P NMR (Table VI), and molecular weight measurements require the all-trans (D_{2h}) structure analogous to **3**. In the conversion of **1** to **6** by stepwise addition of *t*-BuNC, an intermediate has been observed by ^1H NMR (Figure 4) which has methyl resonances distinct from those of **1** and **6**. Several important facts may be gleaned from this titration. First, the NMR integration of *t*-Bu vs. Me shows that the intermediate contains only one isocyanide and therefore has the formula $RuCl_2(PO)_2(t\text{-BuNC})$ (**7**). Second, the presence of only one methoxyl resonance in the ^1H NMR

Table V. Unweighted Mean Planes[a]

Plane 1: $0.6457X - 0.7267Y - 0.2344Z + 3.0225 = 0$

defining atoms	dist, Å	nondefining atoms	dist, Å
P(1)	0.057	C(1)	−0.828
P(2)	−0.061	C(2)	0.547
O(1)	−0.062	Cl(1)	−2.353
O(2)	0.059	Cl(2)	2.374
Ru	0.008		

Plane 2: $-0.3602X + 0.0434Y - 0.9319Z + 4.1835 = 0$

defining atoms	dist, Å	defining atoms	dist, Å
P(1)	−0.033	Cl(2)	0.102
Cl(1)	0.101	Ru	−0.120
O(2)	−0.050		

Plane 3: $0.7253X + 0.6862Y - 0.0552Z - 2.9358 = 0$

defining atoms	dist, Å	defining atoms	dist, Å
P(2)	0.046	Cl(2)	−0.113
Cl(1)	−0.116	Ru	0.121
O(1)	0.062		

Plane 4: $-0.3869X + 0.9178Y - 0.0894Z - 3.3364 = 0$

defining atoms	dist, Å	nondefining atoms	dist, Å
C(11)	0.009	P(1)	0.069
C(12)	−0.016	O(1)	−0.057
C(13)	0.011	Ru	−0.761
C(14)	0.001	C(1)	0.536
C(15)	−0.009		
C(16)	0.004		

Plane 5: $-0.5088X + 0.8462Y - 0.1587Z - 1.2082 = 0$

defining atoms	dist, Å	nondefining atoms	dist, Å
C(41)	−0.016	P(2)	−0.102
C(42)	0.016	O(2)	0.044
C(43)	−0.006	Ru	0.671
C(44)	−0.005	C(2)	−0.238
C(45)	0.006		
C(46)	0.005		

Plane 6: $0.1217X - 0.9700Y - 0.2103Z + 4.3622 = 0$

defining atoms	nondefining atoms	dist, Å
Ru	O(1)	0.088
C(12)		
C(1)		

Plane 7: $-0.7196X + 0.6653Y - 0.1987Z - 0.8134 = 0$

defining atoms	nondefining atoms	dist, Å
Ru	O(2)	−0.033
C(42)		
C(2)		

Angles[b] between the Mean Planes

planes	angle, deg	planes	angle, deg
1-2	874	2-3	796
1-3	890	4-5	90
1-4	264	4-6	233
1-5	250	5-7	161

[a] The equations of the planes $AX + BY + CZ + D = 0$ are referenced to or on the gonal coordinate system and were calculated by an eigenvector/eigenvalue method. [b] The angles between planes are defined as the acute angle between their normals.

spectrum of **7** at higher fields than in the spectrum of **6** is consistent with the dynamic equilibrium analogous to that for

Table VI. ^1H and ^{31}P NMR Data

compd	$^1H_{OMe}$[a]	$^1H_{t\text{-}Bu}$[a]	$^{31}P\{^1H\}$[b]
PO	6.40		−16.0
$RuCl_2(PO)_2$, **1**	5.60		−16.47
$RuCl_2(PO)_2(CO)$, **4**	6.65		36.97
trans-$RuCl_2(PO)_2(CO)_2$, **3**	6.49		26.72
cis-$RuCl_2(PO)_2(CO)_2$, **5**	6.45		10.60
$RuCl_2(PO)_2(t\text{-BuNC})_2$, **6**	6.42	9.00	33.21
$RuCl_2(PO)_2(t\text{-BuNC})$, **7**	6.60	8.69	
$RuCl_2(PO)_2(t\text{-BuNC})(CO)$, **8**	6.64	8.88	27.82

[a] ^1H NMR spectra were recorded in $CDCl_3$ and values are reported in τ relative to Me_4Si. [b] $^{31}P\{^1H\}$ spectra were measured in CH_2Cl_2 and are reported in values of ppm relative to external H_3PO_4; downfield shifts are positive.

Table VII. Infrared Data

no.	compd	$\nu_{Ru\text{-}Cl}$,[a] cm^{-1}	$\nu_{CO,CN}$,[a] cm^{-1}
1	$RuCl_2(PO)_2$	328[b]	
2	$[RuCl_2(PO)_2]BF_4 \cdot CH_2Cl_2$	368	
3	$RuCl_2(PO)_2(CO)$	342	1962
4	*trans*-$RuCl_2(PO)_2(CO)_2$	334	2000
5	*cis*-$RuCl_2(PO)_2(CO)_2 \cdot CH_2Cl_2$	302, 278	2000, 2060
6	*trans*-$RuCl_2(PO)_2(t\text{-BuNC})_2$	304	2130 (2123[c])
7	$RuCl_2(PO)_2(t\text{-BuNC})$		2080[c]
8	*trans*-$RuCl_2(PO)_2(CO)(t\text{-BuNC})$	324[d]	2178, 2005
	t-BuNC		2145[c]

[a] Measured on mineral oil mulls. [b] Reference 14. [c] Measured on CH_2Cl_2 solution. [d] Weaker bands at 340, 272, and 224 cm^{-1}.

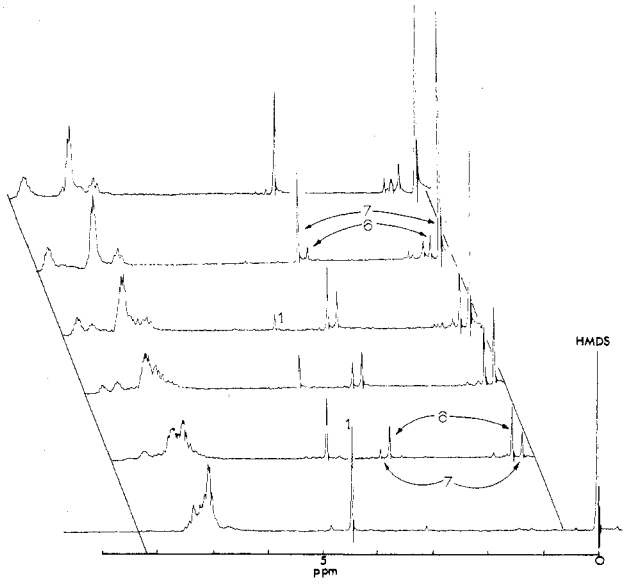

Figure 4. NMR spectral monitor of the titration of $RuCl_2(PO)_2$ (**1**) with *t*-BuNC, yielding $RuCl(t\text{-BuNC})(PO)_2$ (**6**) and *trans*-$RuCl_2(t\text{-BuNC})_2(PO)_2$ (**7**) with HMDS (hexamethyldisiloxane) as a standard.

the monocarbonyl (eq 1). Complex **7** was also observed upon the reaction of solutions of **1** and **6**.

The mechanism by which the initially cis phosphines in **1** rearrange to mutually trans positions for **3** and **6** is likely to involve a trigonal-bipyramidal intermediate; however, an equatorial bidentate chelate (required by mutually trans chlorides) would be strained because of the small chelate bite angle. Alternatively, the cis to trans rearrangement could occur *subsequent* to the association of the incoming ligand (CO, *t*-BuNC) via a strain-free trigonal bipyramid which contains only monodentate PO ligands (eq 3).

The monoadducts of **1**, **4**, and **7** are in rapid equilibrium with a five-coordinate intermediate which is easily formed via

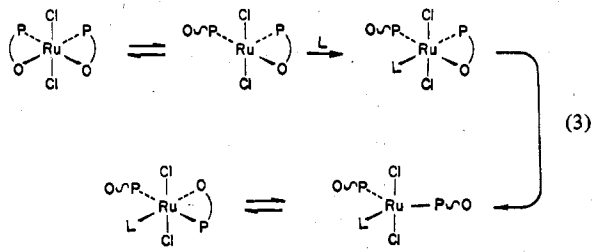

(3)

dissociation of the remaining ether ligand. This coordinatively unsaturated intermediate may then react with other ligands to yield bis adducts, **3** and **6**, in the kinetically favored trans geometry. Alternatively, this intermediate can react in a slower step, involving substantial rearrangement of the coordination sphere to yield to cis,trans,cis product, **5**. Compound **5** is thermodynamically more stable than the all-trans adduct **3**, and conversion of **5** to **3** can only be accomplished photochemically. Further confirmation of the incipient coordinative unsaturation of complexes of the type **4** and **7** is demonstrated by the reaction of *t*-BuNC with **4** to give the mixed isocyanide–carbonyl complex $RuCl_2(PO)_2(t\text{-BuNC})(CO)$ (**8**), which is assigned the all-trans geometry (Tables VI and VII).

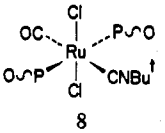

8

The reactions of **1** with other ligands have been looked at briefly. Sulfur dioxide, hexafluoro-2-butyne, ethylene, carbon disulfide, and Et_4NCl do not react. Acetonitrile and nitric oxide do react to give yellow products which contain the added ligand; the former is likely to be $Ru(PO)_2(MeCN)_2Cl_2$, analogous to $Ru(PPh_3)_2(MeCN)_2Cl_2$ isolated by Gilbert and Wilkinson.[45]

Discussion

These results are completely in accord with the recently published work or Barnard et al.[53] In brief, they find that complexes of the type *all-trans*-$Ru(PR_3)_2(CO)_2Cl_2$ analogous to **3** and **6** thermally isomerize to the cis dicarbonyl analogous to **5**. Furthermore, they note that this cis dicarbonyl reverts to the all-trans photochemically. Our systems differ in having the ether group available to compete for vacant coordination sites. In their case, the *all-trans*-$Ru(PR_3)_2(CO)_2Cl_2$ can be reversibly converted to a monocarbonyl which they suggest is a dimer, $[Ru(PR_3)_2(CO)Cl_2]_2$, although few data on this latter complex are presented.[54] Apparently in our case, the ether group competes effectively with potentially bridging chlorides to prevent the formation of the μ-dichloro dimer.

The hinging action of the PO chelate is relevant to other work on anisole phosphine complexes. Shaw and co-workers[9] have reported that the rates of oxidative addition of CH_3I to complexes of the type $Ir(PR_2Ar)_2(CO)Cl$ were greatly enhanced for Ar = *o*-$PhOCH_3$ relative to more basic phosphines. If the rate of oxidative addition were reliant solely on the ligand basicities, complexes of the more basic phosphine would be more reactive. These workers invoked a neighboring group effect wherein the methoxy group in the ortho position binds to the iridium(I), enhancing its nucleophilicity and subsequently dissociating after attack by CH_3I on the metal center. The present work illustrates the feasibility of this mechanism.

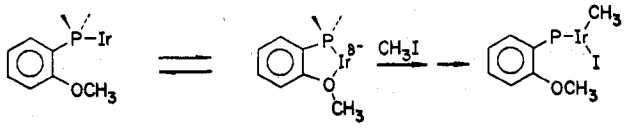

Lastly, the chemistry and structure of **1** have a bearing on the mechanism of the Monsanto L-Dopa synthesis which has as its crucial step the asymmetric hydrogenation of a prochiral olefin by a rhodium complex of a chiral phosphine. After screening of a variety of optically active phosphines, PRR′R″, for the effectiveness of their rhodium complexes in the asymmetric induction, Knowles et al. found that *o*-anisolephosphines were most effective, in particular *o*-(methyl(cyclohexyl)phosphino)anisole.[5] The stereoselectivity of rhodium complexes of this ligand was originally attributed to the ability of the methoxy group to bind to the *substrate* in addition to the phosphorus atom binding the metal, although the possibility of chelate formation has been noted. More recent work by the Monsanto group concerns the improved reliability of the bis(phosphine) ligand *R,R*-PPh(*o*-$PhOCH_3$)CH_2CH_2PPh(*o*-$PhOCH_3$)(diPAMP)

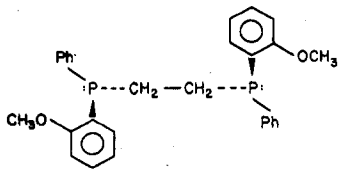

which contains two anisole groups.[8] Also included in this report is a brief description of a structural study of the complex Rh(COD)(diPAMP)BF_4 (COD = 1,5-cyclooctadiene).

Complexes of the type $Rh(COD)(PR_3)_2^+$ are catalytically active only after removal (by hydrogenation) of the chelating olefin to form complexes of the type $Rh(phosphine)_2(solvent)_2^+$[55] where, in the Monsanto process, the solvent is often ethanol. We and others have demonstrated that the ether group competes effectively with ethanol as ligands for ruthenium(II) and rhodium(I)[41] and -(III)[18] (complex **1** is prepared in boiling ethanol). In light of these results, it is plausible that the Monsanto catalysts contain phosphine–ether chelates in solution and that these P–O chelates dissociate in a hemilabile manner. It is logical to conclude that the steroselectivity of these catalyst systems may derive in part from the chelating nature of the P–O ligands which renders the phosphine more rigid and thus more stereochemically discriminating than their freely rotating counterparts.

Summary

(1) The title complex, **1**, is hexacoordinate and contains cis chelates and trans chlorides. The Ru–O distances are very long and the Ru–P distances are close to those observed for five-coordinate ruthenium phosphines. The reaction of **1** with CO yields three complexes, a monocarbonyl which is stereochemically nonrigid, a trans dicarbonyl and a cis dicarbonyl. All of these can be interconverted.

(2) *tert*-Butyl isocyanide reacts analogously to CO, and the mono and trans adducts are observed. The titration of **1** with *t*-BuNC demonstrates that the equilibrium constants for the two additions are comparable.

(3) **1** and its reactivity represent a good model for a hemilabile chelate complex.

(4) Our evidence supports earlier contentions of the action of phosphine anisoles by ourselves and Shaw's group[9a] and suggests that the hinging action of these chelates may be operative in the Monsanto catalytic L-Dopa synthesis.

Acknowledgment. We thank Dr. G. B. Robertson for the use of the X-ray facilities, Dr. M. A. Bennett for helpful comments on the manuscript, and Ms. Janet Hope for assistance with the electrochemical measurements.

Registry No. **1**, 70981-08-7; **2**, 70912-38-8; **3**, 70912-39-9; **4**, 53897-22-6; **5**, 70981-09-8; **6**, 70912-40-2; **7**, 70912-41-3; **8**, 70912-42-4.

Supplementary Material Available: A listing of structure factor amplitudes for $Ru(PO)_2Cl_2$ and Tables VIII, distances and angles within the phenyl rings, and IX, intra- and intermolecular nonbonded

contacts in $RuCl_2(P(C_6H_5)_2(o\text{-}C_6H_4OCH_3))_2 \cdot CH_2Cl_2$ (20 pages). Ordering information is given on any current masthead page.

References and Notes

(1) Addresses for correspondence: J.C.J., Department of Inorganic Chemistry, The University of Bristol, BS8 1TS, England; T.B.R., School of Chemical Sciences, University of Illinois, Urbana-Champaign, Urbana, Ill. 61801.
(2) B. R. James, "Homogeneous Hydrogenation", Wiley-Interscience, New York, 1973.
(3) K. A. Taylor, *Adv. Chem. Ser.*, **No. 70**, 195 (1968).
(4) T. B. Dang and H. B. Kagan, *J. Am. Chem. Soc.*, **94**, 6429 (1972).
(5) W. S. Knowles, M. J. Sebacky, and B. D. Vineyard, *Adv. Chem. Ser.*, **No. 132** (1974), and references therein.
(6) T. Hayashi, T. Mise, S. Mitachi, K. Yamamoto, and M. Kumada, *Tetrahedron Lett.*, 1133 (1976).
(7) T. B. Rauchfuss, F. T. Patino, and D. M. Roundhill, *Inorg. Chem.*, **4**, 652 (1975).
(8) B. D. Vineyard, W. S. Knowles, M. J. Sebacky, G. L. Backman, and D. J. Weinkauff, *J. Am. Chem. Soc.*, **99**, 5946 (1977).
(9) (a) E. M. Miller and B. L. Shaw, *J. Chem. Soc., Dalton Trans.*, 480 (1974); (b) C. E. Jones, B. L. Shaw, and B. L. Turth, *ibid.*, 992 (1974); (c) H. D. Empsall, E. M. Hyde, C. E. Jones, and B. L. Shaw, *ibid.*, 1980 (1974).
(10) T. B. Rauchfuss, unpublished results.
(11) A. R. Hendrickson, R. L. Martin, and N. M. Rhode, *Inorg. Chem.*, **14**, 2980 (1975).
(12) F. T. Patino, M.S. Thesis, Washington State University, Pullman, Wash., 1975.
(13) D. T. Cromer and J. B. Mann, *Acta Crystallogr., Sect. A*, **24**, 321 (1968).
(14) De Meulenaer and H. Tompa, *Acta Crystallogr.*, **19**, 1014 (1965); N. N. Alcock, *Acta Crystallogr., Sect. A*, **25**, 518 (1969).
(15) M. R. Churchill, *Inorg. Chem.*, **12**, 1213 (1973).
(16) G. B. Robertson and P. O. Whimp, *Inorg. Chem.*, **13**, 1047 (1974).
(17) C. K. Johnson, Report ORNL-3794, Oak Ridge National Laboratory, Oak Ridge, Tenn., 1965.
(18) R. Graziani, G. Bombieri, L. Volponi, C. Panattoni, and R. J. H. Clark, *J. Chem. Soc. A*, 1236 (1969).
(19) B. L. Haymore and J. A. Ibers, *Inorg. Chem.*, **14**, 3060 (1975).
(20) B. L. Haymore and J. A. Ibers, *J. Am. Chem. Soc.*, **97**, 5369 (1975).
(21) K. A. Raspin, *J. Chem. Soc. A*, 461 (1969).
(22) S. R. Fletcher and A. C. Skapski, *J. Chem. Soc., Dalton Trans.*, 635 (1972).
(23) S. J. LaPlaca and J. A. Ibers, *Inorg. Chem.*, **4**, 778 (1965).
(24) A. C. Skapski and P. C. H. Troughton, *Chem. Commun.*, 1230 (1968).
(25) T. V. Ashworth, E. Singleton, and M. Laing, *J. Chem. Soc., Chem. Commun.*, 875 (1976).
(26) A. C. Skapski and F. A. Stephens, *J. Chem. Soc., Dalton Trans.*, 390 (1974).
(27) A. I. Gusev, G. G. Aleksandrov, and Y. T. Struchkov, *Zh. Strukt. Khim.*, **14**, 685 (1973); *J. Struct. Chem. (Engl. Transl.)*, **14**, 633 (1973); I. S. Kolomnikov, A. I. Gusev, G. G. Aleksandrov, T. S. Lobeeva, Y. T. Struchkov, and M. E. Vol'pin, *J. Organomet. Chem.*, **59**, 349 (1973).
(28) B. Cetinkaya, M. F. Lapport, G. M. McLaughlin, and K. Turner, *J. Chem. Soc., Dalton Trans.*, 1591 (1974).
(29) L. Pauling, "Nature of the Chemical Bond", 3rd ed., Cornell University Press, Ithaca, N.Y., 1960, pp 224, 249.
(30) A. J. P. Domingos, B. F. G. Johnson, J. Lewis, and G. M. Sheldrick, *J. Chem. Soc., Chem. Commun.*, 912 (1973).
(31) F. A. Cotton, J. G. Norman, A. Spencer, and G. Wilkinson, *Chem. Commun.*, 967 (1971).
(32) M. J. Bennett, K. G. Caulton, and F. A. Cotton, *Inorg. Chem.*, **8**, 1 (1969).
(33) S. Komiya, T. Ito, M. Cowie, A. Yamamoto, and J. A. Ibers, *J. Am. Chem. Soc.*, **97**, 2567 (1975).
(34) J. V. McArdle, A. J. Schultz, C. J. Corden, and R. Eisenberg, *Inorg. Chem.*, **12**, 1676 (1973).
(35) A. J. Schultz, R. L. Henry, J. Reed, and R. Eisenberg, *Inorg. Chem.*, **13**, 732 (1974).
(36) J. Rosalky, Ph.D. Thesis, Australian National University, 1975.
(37) F. Piona, J. B. Briaoso, C. Miravitlles, S. Solons, and M-Font-Altaba, *Acta Crystallogr., Sect. B*, **32**, 2660 (1976).
(38) J. Reiding, A. J. Dekok, R. A. G. DeGregg, and C. Romers, *Acta Crystallogr., Sect. B*, **32**, 2643 (1976).
(39) A. Dunand and R. Gerdil, *Acta Crystallogr., Sect. B*, **32**, 1591 (1976).
(40) F. Iwasaki, I. Tancika, and A. Alhara, *Acta Crystallogr., Sect. B*, **32**, 1264 (1976).
(41) N. W. Alcock, J. M. Brown, and J. C. Jeffrey, *J. Chem. Soc., Dalton Trans.*, 583 (1976).
(42) P. S. Hallman, T. A. Stephenson, and G. Wilkinson, *Inorg. Synth.*, **12**, 237 (1970).
(43) J. M. Jenkins, M. S. Lupin, and B. L. Shaw, *J. Chem. Soc. A*, 1787 (1966).
(44) R. A. Head, J. F. Nixon, J. R. Swain, and C. M. Woodward, *J. Organomet. Chem.*, **76**, 393 (1974).
(45) J. D. Gilbert and G. Wilkinson, *J. Chem. Soc. A*, 1749 (1969).
(46) S. D. Robinson and G. Wilkinson, *J. Chem. Soc. A*, 300 (1966).
(47) M. A. Bennett, R. N. Johnson, and I. B. Tomkins, *Inorg. Chem.*, **13**, 346 (1974).
(48) J. Chatt and R. G. Hayter, *J. Chem. Soc.*, 896 (1961).
(49) L. F. Warren and M. A. Bennett, *Inorg. Chem.*, **15**, 3126 (1976).
(50) J. Chatt, G. J. Leigh, and D. M. P. Mingos, *J. Chem. Soc. A*, 1674 (1974).
(51) M. S. Lupin and B. L. Shaw, *J. Chem. Soc. A*, 741 (1968).
(52) M. A. Bennett, R. N. Johnson, and I. B. Tomkins, *Inorg. Chem.*, **13**, 346 (1974).
(53) C. F. J. Barnard, J. A. Daniels, J. Jeffrey, and R. J. Mawby, *J. Chem. Soc., Dalton Trans.*, 953 (1976).
(54) See B. R. James, L. D. Markham, B. C. Hui, and G. L. Rempel, *J. Chem. Soc., Dalton Trans.*, 2247 (1973).
(55) R. R. Schrock and J. A. Osborne, *J. Am. Chem. Soc.*, **98**, 2134 (1976).

Contribution from the Department of Chemistry, University of Natal, Durban 4001, Republic of South Africa, and the National Chemical Research Laboratory, CSIR, Pretoria 0001, Republic of South Africa

Structures of Five-Coordinate Dinitrosyls of Manganese. 3. Dinitrosyltris(dimethyl phenylphosphonite)manganese(I) Tetrafluoroborate, $[Mn(NO)_2\{P(OCH_3)_2C_6H_5\}_3]BF_4$

MICHAEL LAING,* ROLF H. REIMANN, and ERIC SINGLETON

Received February 13, 1979

The crystal structure of dinitrosyltris(dimethyl phenylphosphonite)manganese(I) tetrafluoroborate, $[Mn(NO)_2\{P(OCH_3)_2C_6H_5\}_3]BF_4$, has been determined by X-ray diffraction. The compound crystallizes from ether/CH_2Cl_2 in the monoclinic space group $P2_1/c$, with a = 14.585 (5) Å, b = 13.085 (5) Å, c = 18.610 (10) Å, β = 110.45 (5)°, V = 3327 Å^3, ρ_{obsd} = 1.41 g cm^{-3}, and Z = 4. The structure was solved by conventional Patterson and Fourier methods and refined by block-diagonal least squares to R = 0.064 for 2999 reflections with $I > 2.0\sigma(I)$. The coordination about the manganese is trigonal bipyramidal with the two NO groups equatorial. The two axial phosphonite ligands bend *toward* the equatorial phosphonite ligand. The NO groups are ordered and are bent in toward each other. The atoms of the $\{Mn(NO)_2P_{eq}\}$ group are coplanar. Bond lengths and angles of interest are as follows: Mn–P_{ax} = 2.303, 2.312 (5) Å; Mn–P_{eq} = 2.356 (5) Å; Mn–N = 1.649, 1.649 (10) Å; N–O = 1.18, 1.19 (1) Å; Mn–N–O = 168, 170 (1)°; P_{ax}–Mn–P_{ax} = 175.5 (5)°; P_{ax}–Mn–P_{eq} = 87.7, 89.8 (5)°; N–Mn–N = 116.5 (5)°; O–Mn–O = 107.4 (5), N–Mn–P_{eq} = 114.0, 129.4 (5)°. Short nonbonded separations are as follows: P_{ax}···N = 2.82, 2.82, 2.85, 2.92 Å; P_{ax}···P_{eq} = 3.23, 3.29 Å.

Introduction

Although neutral nitrosyl complexes of the 3d transition metals are well-known,[1] relatively few cationic species have been prepared.[2] The compound $[Mn(NO)_2\{P(OCH_3)_2C_6H_5\}_3]BF_4$ was readily made[3] from $[Mn(NO)_2\{P(OCH_3)_2C_6H_5\}_2Cl]$, a compound of known crystal structure.[4] Although the manganese atom has the same formal electron count in these two complexes, the frequencies of the nitrosyl stretching

* To whom correspondence should be addressed at the University of Natal.

0020-1669/79/1318-2666$01.00/0